Dowhuszko, Alexis A.; Ilter, Mehmet C.; Hamalainen, Jyri

# Visible Light Communication System in Presence of Indirect Lighting and Illumination Constraints

*Published in:*
2020 IEEE International Conference on Communications, ICC 2020 - Proceedings

*DOI:*
10.1109/ICC40277.2020.9148675

Published: 01/06/2020

*Document Version*
Peer reviewed version

# Visible Light Communication system in presence of indirect lighting and illumination constraints

Alexis A. Dowhuszko[1], *Senior Member, IEEE*, Mehmet C. Ilter[2], and Jyri Hämäläinen[3], *Senior Member, IEEE*
[1]Centre Tecnològic de Telecomunicacions de Catalunya (CTTC/CERCA), Castelldefels (Barcelona), Spain
[2]Department of Signal Processing and Acoustics, Aalto University, Espoo, Finland
[3]Department of Communications and Networking, Aalto University, Espoo, Finland
Email: alexis.dowhuszko@cttc.es; mehmet.ilter@aalto.fi; jyri.hamalainen@aalto.fi

***Abstract*—Visible Light Communication (VLC) systems are designed to provide illumination and data services simultaneously. To achieve this goal, LED lamps are usually deployed on the room ceilings, in order to maximize the chances of having Line-of-Sight (LoS) connectivity between the VLC transmitter and the random locations that the VLC receiver can take. In an early stage of adoption, where the cost of LED lighting fixtures enabled with VLC technology will not be suitable for ultra-dense deployments, it is expected that only one VLC transmitter is placed per room. In this situation, the use of *direct illumination* may have serious problems to satisfy the illumination constraints and provide a homogeneous data rate coverage. Moreover, the use of a single powerful LED lamp per room may create discomfort glare effect to users and over-exposure problems in areas of the room at which the light beam is directed. In order to address these problems, this paper studies the data rate that VLC technology can achieve with *indirect illumination*. That is, when the LED lamp is pointing upwards, and the VLC user receives the optical signal that is reflected back from the ceiling. Obtained simulation results show that indirect illumination provides a more homogeneous data rate coverage when compared to direct case, while simultaneously verifying the illumination constraints in most of the places that the VLC receiver may take in the room.**

***Index Terms*—Visible Light Communication, Illumination Constraints, Phosphor-Converted LEDs, Optical OFDM, Data Rate, Mean Illuminance, Illuminance Uniformity.**

## I. Introduction

Ubiquitous use of Light-Emitting Diodes (LEDs), originally deployed to provide illumination, paves the way for the adoption of the new communication paradigm that is known as Visible Light Communication (VLC). The popularity of VLC technology stems from the license-free electromagnetic spectrum that is used (visible light) and the possibility to control the interference that is created in ultra-dense small cell deployments, which are notably in contrast to what is currently observed in radio systems using the over-crowded Radio Frequency (RF) bands [1]. Moreover, as optical wireless signals cannot penetrate through opaque obstacles such as walls and courtains, VLC technology also offers reliable and secure communication for indoor areas. From this perspective, VLC systems seem a promising complementary solution to RF communications, particularly for the Beyond 5G landscape [2].

In order to provide communication and lighting services simultaneously, the data-carrying signal is used to modulate the light intensity of the LED at a speed that is imperceptible to the human eye, but that can be properly detected by a Photodetector (PD). This way, a low-cost Intensity Modulation (IM)/Direct Detection (DD) communication link results [3]. Since the intensity of light can only take real-positive values, conventional Orthogonal Frequency-Division Multiplexing (OFDM) cannot be used directly, as in RF systems [4]. Therefore, to obtain a waveform that is suitable for an IM/DD link, Optical OFDM schemes should be utilized instead. For example, in DC-biased Optical (DCO)-OFDM, the desired unipolar baseband signal is obtained by first forcing the Hermitian symmetry condition on the vector of input QAM symbols that feeds the Inverse Fast Fourier Transform (IFFT), and then clipping the negative values that remain after adding the selected DC-level [5].

One of the main drawbacks of VLC systems is related to the Line-of-Sight (LoS) blockage that may happen when a moving obstacle is placed between the transmitter and receiver. To address this problem, the authors of [6]–[8] proposed to use multiple transmission points to provide diversity in terms of LoS links, assuming that few LED lamps can be placed on the room ceiling to provide *direct illumination* towards the PDs that are placed beneath. Similarly, the authors of [9] studied the benefits of applying different LED lamp deployment patterns on the ceiling to achieve a better coverage uniformity in the room. However, in all these VLC scenarios in which direct illumination is used, over-exposure problems may emerge on those room areas in which the LED light beams are focused, or the eyes of the VLC users may suffer from the glare effect that strong directive light generates if not properly distributed [10].

A simple way to address this issue consists in using *indirect illumination*, such that the LED light is reflected back from the room ceiling to distribute light more uniformly [11], [12]. In this context, a reflective surface design framework was proposed in [13] to reach the desired illumination uniformity. Unfortunately, only few papers have studied the performance of a VLC system that is designed for Non-Line-of-Sight (NLoS) transmission from the beginning. For example, some experimental results over NLoS links were presented in [14] when using optical mirrors deployed in the room, or when covering the room floor with a special material that improves its mean spectral reflectance coefficient [15].

Motivated by these facts, this paper studies the achievable data rate of a VLC system with indirect illumination, where the LED lamp is pointing upwards and the VLC user receives

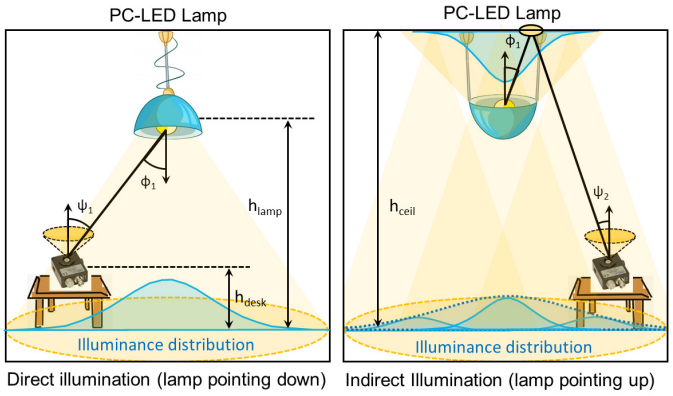


Fig. 1: Indoor VLC system using a PC-LED lamp to provide optical wireless access in presence of direct illumination (left-hand side) and indirect illumination (right-hand side). Blue (Gaussian-like) functions show the distribution of the optical power that is expected in the different locations.

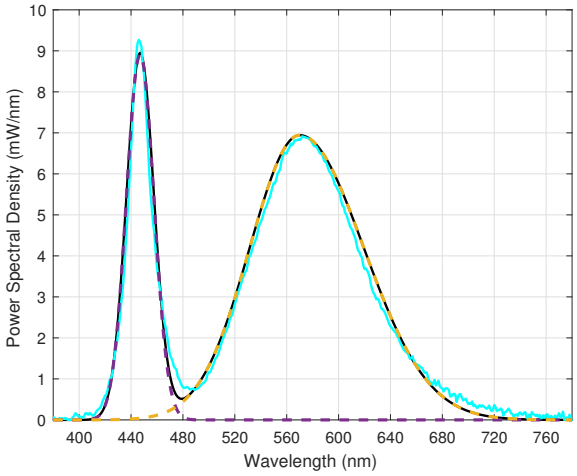


Fig. 2: Measured SPD of PC-LED Bridelux Ledtech (solid cyan line) [16], estimated SPD of light emitted by the B-Chip (dashed violet line), Y-Phosphor (dashed yellow line), and the aggregate light that results when combining both sources (solid black line). PSD is normalized to have unitary radiated power.

the light that is reflected back from the ceiling. The effect that indirect illumination has on both data rate coverage and illuminance uniformity will be characterized in detail, trying to identify the percentage of the room area in which the illumination requirements (set by regulations) are verified. It will be shown that indirect illumination is a good option for an early phase of deployment, as a single VLC-enabled lamp is expected to be placed initially per-room due to the high cost that this new technology will have until its massive adoption.

The rest of the paper is organized as follows: The different parts of the VLC system are described in Section II, including the LED transmitter, optical wireless channel, and PD receiver. The Key Performance Indicators (KPIs), such as illuminance and achievable data rate, are explained in Section III, whereas the corresponding simulation results are shown in Section IV. Finally, conclusions are drawn in Section V.

## II. System Model

Consider the VLC system model presented in Fig. 1, consisting of a Phosphor-Converted (PC) LED that is placed in the center of the room at height $h_{\rm lamp}$, a plain ceiling surface with known spectral reflectance at height $h_{\rm ceil}$, and a PD on top of a desk at $h_{\rm desk}$ meters from the floor. The *direct illumination* scenario is shown on the left-hand side of Fig. 1, where the PC-LED lamp is pointing downwards and most of the optical power on the PD arrives through LoS propagation from transmitter to receiver. On the other hand, the *indirect illumination* case is shown on the right-hand side of Fig. 1, where the PC-LED lamp is pointing upwards, and the optical power that reaches the PD is first reflected on the ceiling.

For the sake of simplicity, only the downlink direction of communication is considered (note that for uplink, visible light should be replaced by infra-red). All the signal processing that is needed to obtain the DCO-OFDM waveform is implemented in the VLC transmitter, where the QAM symbols that are allocated on the subcarriers are forced to verify the Hermitian Symmetry property. After the IFFT block, a DC-level is added and the negative values of the resulting time-domain signal are clipped. In order to model the End-to-End (E2E) response of the VLC link, the three main blocks (*i.e.*, VLC transmitter, optical wireless channel, and VLC receiver) are now described.

### A. Spectral Power Distribution of PC-LEDs

Phosphor Converted LEDs consists of a Blue (B)-Chip and a Yellow (Y)-phosphor layer, whose interaction generates white light with a Correlated Color Temperature (CCT) that depends on the balance between the area of the Spectral Power Distribution (SPD) of the light generated by the B-Chip, $S_{\rm o}^{(\rm b)}(\lambda)$, and the area of the SPD of the green-yellow-red light converted from the Y-phosphor layer, $S_{\rm o}^{(\rm p)}(\lambda)$.

Most data sheets of PC-LEDs, which are designed for illumination, usually provide low-quality plots of the relative radiant SPD of the aggregate white light that is generated, *i.e.*,

$$G_{\rm rel}(\lambda)=\frac{S_{\rm o}^{(\rm w)}(\lambda)}{\max_\lambda\{S_{\rm o}^{(\rm w)}(\lambda)\}},\ S_{\rm o}^{(\rm w)}(\lambda)=S_{\rm o}^{(\rm b)}(\lambda)+S_{\rm o}^{(\rm p)}(\lambda). \quad (1)$$

Nevertheless, the marginal distribution functions for $S_{\rm o}^{(\rm b)}(\lambda)$ and $S_{\rm o}^{(\rm p)}(\lambda)$ are needed, since the B-Chip and Y-Phosphor have a different time response that affect notably the frequency response of the PC-LED [17] and, consequently, the achievable data rate of the DCO-OFDM VLC system. For this, we apply the approach proposed in [18] and assume that the SPD of the B-Chip (Y-Phosphor) can be accurately approximated by a (an) symmetric (asymmetric) Gaussian function, *i.e.*,

$$S_{\rm o}^{(\rm b)}(\lambda)\ \approx\ A_1\exp\Big\{-\Big(\frac{\lambda-\mu_1}{\sigma_1}\Big)^2\Big\}, \quad (2)$$

$$S_{\rm o}^{(\rm p)}(\lambda)\ \approx\ A_2\exp\Big\{-\Big(\frac{\lambda-\mu_2}{\sigma_2\big[1+{\rm sign}(\lambda-\mu_2)\,\alpha\big]}\Big)^2\Big\}, \quad (3)$$

where $A_1$ ($A_2$) is proportional to optical intensity radiated by the B-Chip (Y-Phosphor) at peak wavelength $\mu_1$ ($\mu_2$), $\sigma_1$ ($\sigma_2$) is proportional to the Full Width at Half Maximum (FWHM) optical power emitted by the B-Chip (Y-Phosphor), $\alpha$ is the asymmetric factor for the optical radiation emitted by the Y-Phosphor, and ${\rm sign}(x)$ equals 1 for $x\geq 0$ and $-1$ otherwise.

TABLE I: Curve fitting parameters of the Gaussian functions that best fit the measured SPD of PC-LED Bridelux Ledtech (4440 K) [16].

| | **Intensity** [mW] | **Peak $\lambda$** [nm] | **Std. Dev.** [nm] | **Asymmetric factor** |
|---|---|---|---|---|
| **Blue Chip** | $A_1 = 8.9126$ | $\mu_1 = 447$ | $\sigma_1 = 15$ | — |
| **Yellow Phosphor** | $A_2 = 6.9436$ | $\mu_2 = 570$ | $\sigma_2 = 62$ | $\alpha = 0.1240$ |

The parameters that minimize the mean square error between the actual measurements (solid cyan line) and the curve-fitting approximation (solid black line) for the PC-LED Bridelux Ledtech [16] are listed in Table I. In addition, the estimated SPD for the B-Chip (dashed violet line) and Y-Phosphor (dashed yellow line) are also shown in Fig. 2. Though the area under $S_{\rm o}^{(\rm w)}(\lambda)$ has been normalized to 1 W, the actual transmit power of the PC-LED lamp is $P_{\rm led} = 56$ W.

### *B. Optical Wireless Channel Model*

Different channel models have been proposed in the literature to characterize the indoor propagation of visible light signals. This paper focuses on two of them, which only considers the effect of the light source and the LoS link in *direct illumination*, and the effect of the light source and the (first-order reflected) NLoS link in *indirect illumination*. The effect of higher-order reflections on walls, floor, and/or other obstacles that may be place in the room is neglected.

*1) Direct illumination (LoS propagation):* In the LoS channel model, the PC-LED is considered as a source of light with a Lambertian radiation pattern; therefore, the DC gain of the optical channel between the LED transmitter and the PD receiver can be written as [19]

$$H_{\rm led,pd}^{\rm dir}(0) = \begin{cases} \dfrac{(m+1)A_{\rm pd}}{2\pi {d_1}^2}\cos^m(\phi_1)\cos(\psi_1), & 0 \le \psi_1 \le \Psi_{\rm c}, \\ 0, & \psi_1 > \Psi_{\rm c}, \end{cases} \tag{4}$$

where $m$ is the Lambert index of the PC-LED, $A_{\rm pd}$ [m$^2$] is the physical area of the PD, $\phi_1$ [rad] and $\psi_1$ [rad] are the angle of irradiance and incidence of the LoS link, respectively, $d_1$ [m] is the distance between transmitter and receiver, and $\Psi_{\rm c}$ [rad] is the Field of View (FOV) semi-angle of the PD. In practice, the Lambert index of the LED can be computed from $m = -1/\log_2\left[\cos(\theta_{\rm max})\right]$, where $\theta_{\rm max}$ [rad] defines the source radiation semi-angle at half power of the PC-LED.

Finally, the spectral optical power of the light that reaches the PD in case of direct illumination is given by

$$p_{\rm o,pd}^{\rm dir}(\lambda) = P_{\rm led}\, H_{\rm led,pd}^{\rm dir}(0)\, S_{\rm o}^{(\rm w)}(\lambda), \tag{5}$$

where $P_{\rm led}$ [W] is the total radiant power of the PC-LED.

*2) Indirect illumination (NLoS propagation):* To model the optical wireless channel between LED transmitter and PD receiver after a first-order reflection on the ceiling, the ceiling area must be divided into (small) non-overlapping reflecting elements of size $A_{\rm ref}$ [20]. Then, the DC gain of the optical channel with indirect illumination can be written as

$$H_{\rm led,pd}^{\rm indir}(0) = \sum_i H_{{\rm led},i}^{\rm dir}(0)\, H_{i,\rm pd}^{\rm dir}(0), \tag{6}$$

where $i$ is the index of each of the (small-sized) reflecting elements in which the ceiling surface is divided, and

$$H_{{\rm led},i}^{\rm dir}(0) = \frac{(m+1)A_{\rm ref}}{2\pi {d_1}^2}\cos^m(\phi_1)\cos(\psi_1), \tag{7}$$

$$H_{i,\rm pd}^{\rm dir}(0) = \frac{A_{\rm pd}}{\pi {d_2}^2}\cos(\phi_2)\cos(\psi_2), \qquad 0 \le \psi_2 \le \Psi_{\rm c}, \tag{8}$$

are the DC gain of the direct links between LED and reflecting element $i$, and between reflecting element $i$ and PD, respectively. In (7)-(8), $\phi_1$ and $\psi_1$ are the angle of irradiance and incidence of the first link, whereas $\phi_2$ and $\psi_2$ are the angle of irradiance and incidence of the second link.

In case of indirect illumination, the spectral optical power of the light that reaches the PD after the ceiling reflection is

$$p_{\rm o,pd}^{\rm indir}(\lambda) = P_{\rm led}\, H_{\rm led,pd}^{\rm indir}(0)\, S_{\rm o}^{(\rm w)}(\lambda)\, \rho_{\rm ceil}(\lambda), \tag{9}$$

where $\rho_{\rm ceil}(\lambda)$ is the reflectance of the ceiling material that is shown in Fig. 3 (solid blue line) [20].

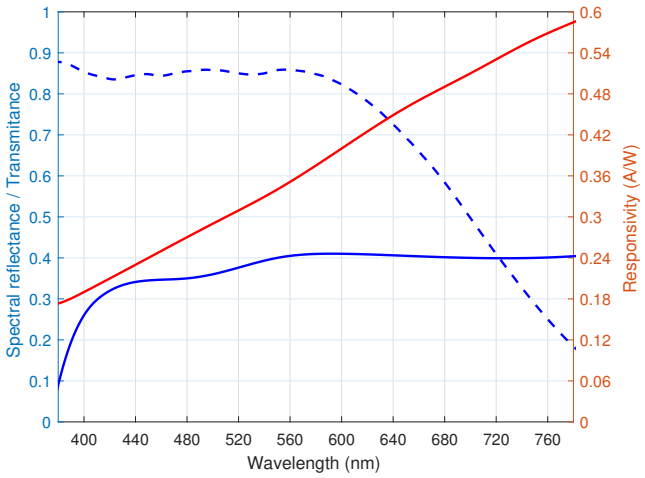


Fig. 3: Spectral reflectance of ceiling material (solid blue line) [20], transmitance of FGS900 visible light optical passband filter (dashed blue line) [21], and responsivity of PDA100A2 Photodetector (solid red line) [22].

### *C. Signal-to-Noise Ratio of the Photodetector Output Signal*

The DC current at the output of the PD is given by

$$i_{\rm pd}^{\rm (in)dir}(0) = \int_{\lambda_{\rm l}}^{\lambda_{\rm u}} p_{\rm o,pd}^{\rm (in)dir}(\lambda)\, {\rm R}_{\rm pd}(\lambda)\, f_{\rm o}(\lambda)\, d\lambda, \tag{10}$$

where ${\rm R}_{\rm pd}(\lambda)$ [A/W] is the responsivity of the PD and $f_{\rm o}(\lambda)$ is the transmitance of the optical passband filter with lower ($\lambda_{\rm l}$) and upper ($\lambda_{\rm u}$) cutoff wavelengths. The responsivity of the PD (solid red line) and the transmitance of the optical passband filter (dashed blue line) can be appreciated in Fig. 3, and have been taken from the data sheets of PDA100A2 [22] and FGS900 [21], both of them manufactured by Thorlabs.

The ambient light that is present in the room (*e.g.*, sunlight that comes through windows), as well as the instantaneous power of the data-carrying signal that reaches the PD, generate shot noise that is added on top of the thermal noise that is introduced by the TransImpedance Amplifier (TIA) embedded into the PD. According to the data sheet of PDA100A2 [22], the noise at the output of the PD is modeled as a Root Mean Square (RMS) aggregate noise voltage $v_{\rm n}$ [V], whose magnitude depends on the TIA gain $G_{\rm tia}$ [V/A] that is selected.

Based on the previously listed considerations, it is possible to show the SNR at the PD output attains the form

$$\Gamma_{\rm pd}(f) = \Gamma_{\rm pd}(0)|H_{\rm w}(f)|^2, \;\; \Gamma_{\rm pd}(0) = \left| \frac{i_{\rm pd}^{\rm (in)dir}(0)\, G_{\rm tia}}{v_{\rm n}} \right|^2, \quad (11)$$

where $H_{\rm w}(f)$ is the frequency response of the PC-LED, which depend on the time constants $\tau_{\rm b}$ and $\tau_{\rm p}$ of the exponential decaying functions that model the response of the B-Chip and Y-Phosphor to the impulse [17]. In this paper, the bandwidth of the DCO-OFDM signal is expected to be narrower than the inverse of the Y-Phosphor time response (*i.e.*, $W \approx 1/\tau_{\rm p}$); then, we assume that $|H_{\rm w}(f)| \approx 1$ for $0 \leq f \leq W$ holds.

## III. Key performance indicators for VLC systems

Two KPIs are defined to study the performance of the proposed VLC system in presence of (in)direct illumination, namely: Illuminance and Achievable Data Rate.

### A. Illuminance constraints to be verified by the VLC system

The illuminance $E_{\rm v}$ is defined as the total luminous flux $\Phi$ incident on a surface per unit area. To compute this parameter for a VLC system with (in)direct illumination (see Fig 1), the SPD of the light that the PD receives should be first weighted by the human eye sensitivity function $V(\lambda)$ and, after that, it should be divided by the physical area of the PD [19], *i.e.*,

$$\Phi = 683 \left[\frac{\rm lm}{\rm W}\right] \int_{380{\rm nm}}^{780{\rm nm}} p_{\rm o,pd}^{\rm (in)dir}(\lambda) V(\lambda)\, d\lambda, \quad E_{\rm v} = \frac{\Phi}{A_{\rm pd}}. \quad (12)$$

Note that the standard luminosity curve is normalized to a peak value of unity at $\lambda = 555$ [nm], and that the tabulated values for $V(\lambda)$ in 5-nm steps appear in Appendix 16.1 of [23].

An average illuminance $E_{\rm avg} = {\rm E}\{E_{\rm v}\} \geq 500$ [Lux] and an illuminance uniformity $U_{\rm E} = \min\{E_{\rm v}\}/E_{\rm avg} \geq 0.6$ should be verified in a standard office room where writing and reading activities are performed [24]. These two KPIs will be used to compare the benefits that indirect illumination provides over direct illumination, when trying to fulfill the illumination constraints that are set by actual regulations. Note that ${\rm E}\{X\}$ denotes the expectation of a random variable $X$.

### B. Achievable data rate of DCO-OFDM VLC link

In DCO-OFDM, the bipolar OFDM signal that results after feeding the IFFT block with an Hermitian symmetric vector of QAM symbols becomes unipolar by adding a suitable DC bias level $x_{\rm B} > 0$. In practice, since the instantaneous amplitude of the DCO-OFDM signal can be approximated as Gaussian distributed, the minimum and maximum amplitudes must be lower- and upper-clipped, respectively, to fulfill the intensity modulation range of the PC-LED. As expected, this process adds clipping noise $n_{\rm clip}$, which is signal-dependent in the time domain, but can be approximated as signal-independent in the frequency domain after applying the Fast Fourier Transform (FFT) in the receiver. In order to minimize the effect of clipping, such that DCO-OFDM signal approximation

$$x_{\rm dco-ofdm}(t) = x_{\rm ofdm}(t) + x_{\rm B} + n_{\rm clip}(x_{\rm B}) \approx x_{\rm ofdm}(t) + x_{\rm B} \quad (13)$$

holds, the optimal clipping level should be selected such that a BER floor does not appear in the performance curves of the different Adaptive and Modulation Coding (AMC) schemes within the SNR (or $E_{\rm b}/N_0$) interval in which each of them should be utilized [5]. Then, the DC-bias can be defined as

$$\gamma_{\rm dc}[{\rm dB}] = 10 \log_{10} \left( \frac{x_{\rm B}^2}{{\rm E}\{x_{\rm dco-ofdm}^2(t)\}} \right) . \quad (14)$$

According to the simulation results reported in [5], the effect of clipping noise for 4-, 16-, 64- and 256-QAM becomes negligible for $\gamma_{\rm dc} = 13\,{\rm dB}$ when the target BER $= 10^{-3}$. Increasing the DC-bias reduces the electrical power of the received AC signal. On the other hand, reducing the DC-bias introduces stronger clipping noise that would affect the system performance (particularly for high-order QAM schemes).

Then, the achievable data rate of the VLC link when using a DCO-OFDM signal to modulate the intensity of the light emitted by the PC-LED is given by

$$R_{\rm dco-ofdm}^{\rm (in)dir} = \int_0^W \log_2 \left( 1 + \frac{\Gamma_{\rm pd}(f)}{\gamma_{\rm dc}} \right) df \approx W \log_2 \left( 1 + \frac{\Gamma_{\rm pd}(0)}{\gamma_{\rm dc}} \right), \quad (15)$$

where $W$ [Hz] is the bandwidth of the DCO-OFDM signal, which is narrower than the frequency response range in which the PC-LED has a flat response. Due to that, $|H_{\rm w}(f)| \approx 1$ for $0 \leq f \leq W$ has been used in the right-hand side of (15) .

## IV. Simulation results

The illuminance and data rate performance of the VLC system with (in)direct illumination is evaluated in a small office scenario with dimension $5\,[{\rm m}] \times 5\,[{\rm m}] \times 3\,[{\rm m}]$, similar to the one presented in [7]. The receiver lies on a desk of height $h_{\rm desk} = 0.85$ [m] that takes random locations on the room, and collects the optical signal that is irradiated by the PC-LED lamp placed on the center of the room at variable height $h_{\rm lamp}$, pointing either downwards (direct illumination) or upwards (indirect illumination). Each PC-LED lamp has a total radiant power $P_{\rm led} = 56\,[{\rm W}]$, an aggregate SPD that is approximated by summing the SPD in (2)-(3) with the parameters listed in Table I, and a viewing angle $\theta_{\rm max} = 60\,[{\rm deg}]$. The spectral reflectance of the ceiling $\rho_{\rm ceil}(\lambda)$, transmitance of the passband optical filter $f_{\rm o}(\lambda)$, and responsivity of the PD that are used to implement the LoS/NLoS VLC link are shown in Fig. 3. The gain of the TIA that is embeded in the PD is $G_{\rm tia} = 750\,[{\rm V/A}]$, and the DC-bias power is $\gamma_{\rm dc} = 13\,{\rm dB}$ larger than the power used to transmit the data-carrying AC component. The bandwidth of the DCO-OFDM signal is $W = 2\,[{\rm MHz}]$, which is similar to the flat response bandwidth of the PC-LED $B_{\rm led} \approx 1/\tau_{\rm p}$ reported in [17]. Finally, the frequency-domain

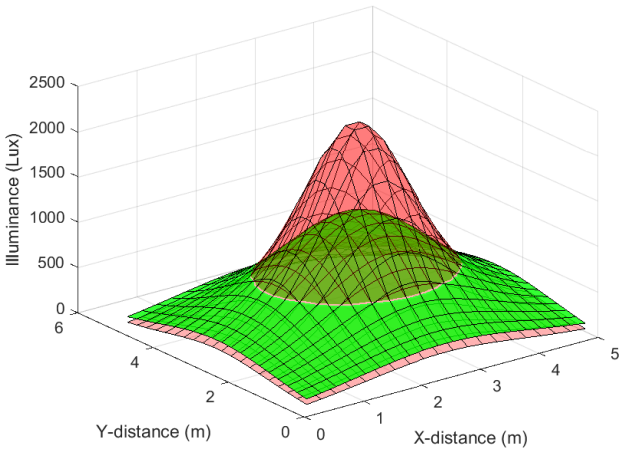


Fig. 4: Illuminance provided by the VLC system in case of direct illumination (red surface) and indirect illumination (green surface). Direct illumination: $P_{\mathrm{led}} = 56\,\mathrm{W}$; $E_{\mathrm{avg}} = 594\,\mathrm{Lux}$; $U_{\mathrm{E}} = 0.15$. Indirect illumination: $P_{\mathrm{led}} = 3 \times 56\,\mathrm{W}$; $E_{\mathrm{avg}} = 562\,\mathrm{Lux}$; $U_{\mathrm{E}} = 0.26$. Both: $h_{\mathrm{lamp}} = 2.5\,\mathrm{m}$.

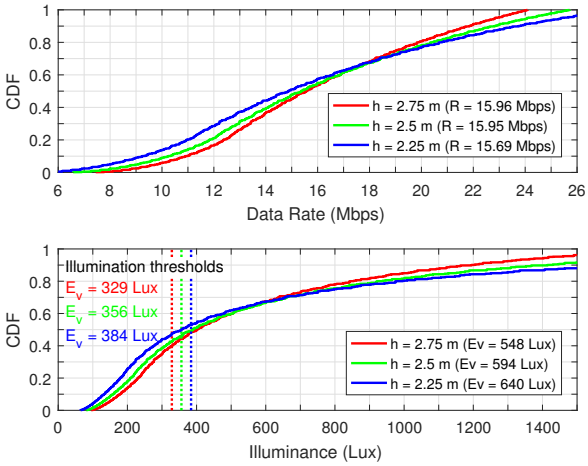


Fig. 6: CDF of achievable data rate (upper) and illuminance (lower) at different room locations with *direct* illumination. Red line: $h_{\mathrm{lamp}} = 2.75\,\mathrm{m}$. Green line: $h_{\mathrm{lamp}} = 2.5\,\mathrm{m}$. Blue line: $h_{\mathrm{lamp}} = 2.25\,\mathrm{m}$. $P_{\mathrm{led}} = 56\,\mathrm{W}$. Mean data rate ($\overline{R}$) and average illuminance ($E_{\mathrm{avg}}$) are included in the legends.

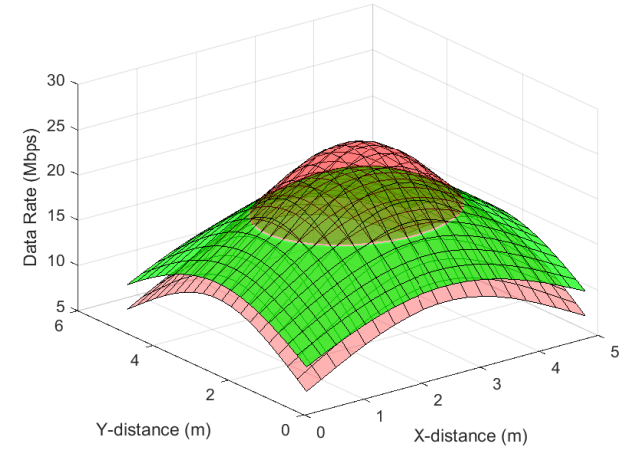


Fig. 5: Data rate achievable by the VLC system in case of direct illumination (red surface) and indirect illumination (green surface). Direct illumination: $P_{\mathrm{led}} = 56\,\mathrm{W}$; $\overline{R} = 15.95\,\mathrm{Mbps}$; $R_{0.1} = 9.98\,\mathrm{Mbps}$. Indirect illumination: $P_{\mathrm{led}} = 3 \times 56\,\mathrm{W}$; $\overline{R} = 16.56\,\mathrm{Mbps}$; $R_{0.1} = 12.31\,\mathrm{Mbps}$. Both: $h_{\mathrm{lamp}} = 2.5\,\mathrm{m}$.

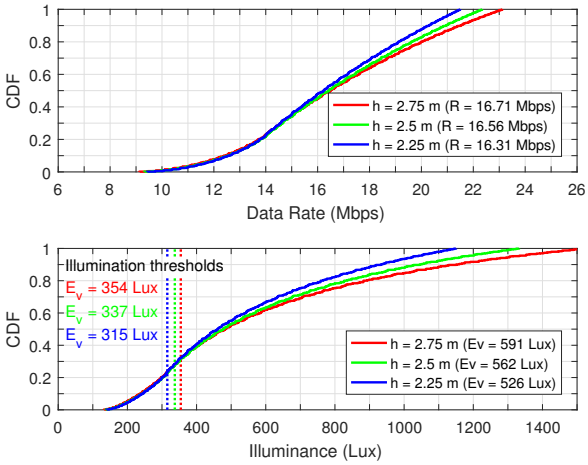


Fig. 7: CDF of achievable data rate (upper) and illuminance (lower) at different room locations with *indirect* illumination. Red line: $h_{\mathrm{lamp}} = 2.75\,\mathrm{m}$. Green line: $h_{\mathrm{lamp}} = 2.5\,\mathrm{m}$. Blue line: $h_{\mathrm{lamp}} = 2.25\,\mathrm{m}$. $P_{\mathrm{led}} = 3 \times 56\,\mathrm{W}$. Mean data rate ($\overline{R}$) and average illuminance ($E_{\mathrm{avg}}$) are included in the legends.

granularity effect for using a discrete number of DCO-OFDM subcarriers is neglected, as well as the impact that the use of Cyclic Prefix (CP) has on the achievable data rate.

Figures 4 and 5 show the illuminance $E_{\mathrm{v}}^{(\mathrm{in})\mathrm{dir}}$ and achievable data rate $R_{\mathrm{dco-ofdm}}^{(\mathrm{in})\mathrm{dir}}$ that the VLC system can provide at the different room locations in case of direct illumination (red surface) and indirect illumination (green surface), respectively. To verify the $E_{\mathrm{avg}} \geq 500\,[\mathrm{Lux}]$ requirement in both cases, one PC-LED lamp and three PC-LED lamps are deployed for direct and indirect illumination, respectively. As expected, the use of indirect illumination enables to provide a more homogeneous service coverage in terms of both illuminance and achievable data rate. For example, according to Fig. 4, though the average illuminance ($E_{\mathrm{avg}}$) does not vary notably when comparing both cases, the illuminance uniformity ($U_{\mathrm{E}}$) with indirect illumination almost double the one observed with direct illumination. Similarly, when comparing the results reported in Fig. 5, the mean data rate ($\overline{R}$) is similar in both cases, whereas the 10-th percentile data rate ($R_{0.1}$) is approximately 25 % larger with indirect illumination than with direct illumination.

Finally, Figs. 6 and 7 show the Cumulative Distribution Function (CDF) for the achievable data rate (upper panel) and illuminance (lower panel) when the bandwidth of the DCO-OFDM signal is $W = 2\,[\mathrm{MHz}]$. In these figures, the effect of placing the LED lamp at different heights (measured from the floor level) is analyzed in detail for both direct and indirect illumination. Firstly, it is possible to see that the larger is $h_{\mathrm{lamp}}$, the higher is the mean data rate ($\overline{R}$) that is

feasible for both direct and indirect illumination. Nevertheless, it is important to notice that this variation is minor. Similarly, when studying the 10-th percentile data rate ($R_{0.1}$), the highest performance with direct illumination was achieved when the PC-LED lamp was placed as close as possible to the ceiling. On the other hand, in case of indirect illumination, the 10-th percentile data rate was not affected by the height of the PC-LED lamp, enabling almost the same *minimum* data rate service within the room regardless $h_{\mathrm{lamp}}$. Finally, concerning the illuminance performance, it is possible to observe that indirect illumination can provide a much more homogeneous coverage than direct illumination. For example, with indirect illumination, the illumination homogeneity ($U_{\mathrm{E}}$) was verified in 65-75 % of the room locations for the different $h_{\mathrm{lamp}}$ that were considered, whereas this value was reduced to less than 50 % of the locations in presence of indirect illumination.

Based on these results, it is possible to conclude that in an initial stage of deployment of VLC technology, it is expected that PC-LED lamps configured to provide indirect illumination indoors will enable a more homogeneous data rate coverage under illumination constraints, which may only be *seldom* violated in those *few corner areas* of the room in which the placement of the VLC user is more unlikely to take place.

## V. Conclusion

We have studied the illuminance and achievable data rate that a DCO-OFDM VLC system is able to provide when only one PC-LED lamp pointing either downwards (direct illumination) or upwards (indirect illumination) can be deployed per office room. To make a reliable estimation of the actual data rate and illuminance that can be provided when the PC-LED lamp is placed at different heights, the optical power spectrum of the PC-LED, the spectral reflectance of the ceiling material, the transmittance of the optical passband filter, and the responsivity of the PD have been taken from measurements reported in scientific papers and data sheets of commercial (electro-)optical devices. Though the use of direct illumination can provide a higher data rate and illuminance than indirect illumination for fixed LED radiant power, it may not represent a good option in an initial phase of deployment of the technology, as many (expensive) VLC-enabled lamps would be needed per room to give an homogeneous data rate coverage while fulfilling the illumination constraints set by regulations. In contrast, if a higher LED radiant power is allowed and a white-painted ceiling material (with good reflectance) is available, the setting of an indirect illumination scenario (by pointing the PC-LED lamps upwards) can provide better data and illumination services, facilitating the massive adoption of VLC technology for future wireless access.

## Acknowledgment

This work has received funding from the Ministry of Science, Innovation, and Universities of Spain under Project TERESA-TEC2017-90093-C3-1-R (AEI/FEDER, UE), from the Catalan government under grant 2017-SGR-01479, and from the ATTRACT project funded by the EC under Grant Agreement 777222.

## References

[1] D. Karunatilaka, F. Zafar, V. Kalavally, and R. Parthiban, "LED based indoor visible light communications: State of the art," *IEEE Commun. Surveys Tutorials*, vol. 17, no. 3, pp. 1649–1678, 3Q 2015.

[2] L. Feng, R. Hu, J. Wang, P. Xu, and Y. Qian, "Applying VLC in 5G networks: Architectures and key technologies," *IEEE Network*, vol. 30, no. 6, pp. 77–83, Nov. 2016.

[3] H. Elgala, R. Mesleh, and H. Haas, "Indoor optical wireless communication: Potential and state-of-the-art," *IEEE Commun. Mag.*, vol. 49, no. 9, pp. 56–62, Sept. 2011.

[4] M. Afgani, H. Haas, H. Elgala, and D. Knipp, "Visible light communication using OFDM," in *Proc. Int. Conf. on Testbeds and Research Infrastructures for the Development of Networks and Communities,*, Mar. 2006, pp. 1–6.

[5] J. Armstrong and B. Schmidt, "Comparison of asymmetrically clipped optical OFDM and DC-biased optical OFDM in AWGN," *IEEE Commun. Letters*, vol. 12, no. 5, pp. 343–345, May 2008.

[6] K. Lee and H. Park, "Modulations for visible light communications with dimming control," *IEEE Photonics Tech. Letters*, vol. 23, no. 16, pp. 1136–1138, Aug. 2011.

[7] A. Dowhuszko and A. Pérez-Neira, "Achievable data rate of coordinated multi-point transmission for visible light communications," in *Proc. Int. Symp. Personal, Indoor, and Mobile Radio Commun.*, Oct. 2017, pp. 1–7.

[8] B. Genovs Guzmán, A. Dowhuszko, V. Gil Jiménez, and A. Pérez-Neira, "Cooperative transmission scheme to address random orientation and blockage events in VLC systems," in *Proc. Int Symp. Wireless Commun. Systems*, Aug. 2019, pp. 351–355.

[9] Shashikant, R. Saini, and A. Gupta, "Comparative analysis of coverage aspects for various LEDs placement schemes in indoor VLC system," in *Proc. Int. Conf. Convergence in Tech.*, Apr. 2017, pp. 487–491.

[10] Z. Zhu, X. Jin, H. Yang, and L. Zhong, "Design of diffuse reflection freeform surface for uniform illumination," *J. Display Technology*, vol. 10, no. 1, pp. 7–12, Jan. 2014.

[11] C.-H. Tsuei, J.-W. Pen, and W.-S. Sun, "Simulating the illuminance and the efficiency of the LED and fluorescent lights used in indoor lighting design," *Opt. Express*, vol. 16, no. 23, pp. 18 692–18 701, Nov. 2008.

[12] A. Dowhuszko, M. Ilter, P. Pinho, and J. Hämäläinen, "The effect of power allocation on Visible Light Communication using commercial phosphor-converted LED lamp for indirect illumination," in *Proc. Int. Conf. Acoustics, Speech and Signal Process.*, May 2020, pp. 1–5.

[13] Z. Zhu, H. Liu, and S. Chen, "The design of diffuse reflective free-form surface for indirect illumination with high efficiency and uniformity," *IEEE Photonics Journal*, vol. 7, no. 3, pp. 1–10, June 2015.

[14] Z. Lu, P. Tian, H. Fu, and et al., "Experimental demonstration of non-line-of-sight visible light communication with different reflecting materials using a GaN-based micro-LED and modified IEEE 802.11 ac," *AIP Advances*, vol. 8, no. 10, pp. 105–017, Oct. 2018.

[15] N. Hassan, Z. Ghassemlooy, S. Zvanovec, P. Luo, and H. Le-Minh, "Non-line-of-sight $2 \times N$ indoor optical camera communications," *Appl. Opt.*, vol. 57, no. 7, pp. B144–B149, Mar. 2018.

[16] J. Roby and M. Aubé, "Lamp spectral power distribution database — Ledtech LED Bridgelux 4440 K," Oct. 2012, url: http://galileo.graphycs.cegepsherbrooke.qc.ca/app.

[17] G. Stepniak, M. Schppert, and C. Bunge, "Advanced modulation formats in phosphorous LED VLC links and the impact of blue filtering," *J. Lightwave Tech.*, vol. 33, no. 21, pp. 4413–4423, Nov. 2015.

[18] R. Zheng, "Luminous efficiency and color rendering of phosphor-converted white LEDs," *J. Light Visual Environ.*, vol. 32, no. 2, pp. 230–233, Jan. 2008.

[19] T. Komine and M. Nakagawa, "Fundamental analysis for visible-light communication system using LED lights," *IEEE Trans. Consumer Electronics*, vol. 50, no. 1, pp. 100–107, Feb. 2004.

[20] K. Lee, H. Park, and J. Barry, "Indoor channel characteristics for visible light communications," *IEEE Commun. Letters*, vol. 15, no. 2, pp. 217–219, Feb. 2011.

[21] Thorlabs, "FGS900 – 25 mm KG3 colored glass bandpass filter, 315-710 nm," Aug. 2011, url: https://www.thorlabs.com/.

[22] ——, "PDA100A2 Si switchable gain detector – User guide," May 2019, url: https://www.thorlabs.com/.

[23] E. Schubert, *Light-Emitting Diodes*, 2nd ed. Cambridge University Press, 2006.

[24] NSAI, "Light and lighting — Lighting of work places — Part 1: Indoor work places," June 2011, Irish Standard I.S. EN 12464.